Preliminary aerodynamic configuration optimization using particle swarm optimization with a multi-component objective function

Nguyen The Hong[1*], Nguyen Van Khoi[1], Pham Trung Dung[2]

[1]Institute of Missile, Academy of Military Science and Technology, 17 Hoang Sam, Nghia Do, Hanoi, Vietnam;
[2]Institute of Missile and Control Engineering, Le Quy Don Technical University, 234 Hoang Quoc Viet, Nghia Do, Hanoi, Vietnam.
[*]Corresponding author: thehong.mta@gmail.com
Received 14 Jun. 2026; Revised 17 Aug. 2026; Accepted 04 Sep. 2026; Published 16 Sep. 2026.
DOI: https://doi.org/10.54939/1859-1043.j.mst.FMC.2026.163-172

ABSTRACT

This paper proposes a preliminary aerodynamic configuration optimization framework coupling particle swarm optimization (PSO) with Missile DATCOM. Eleven-variable Rose baseline geometries are evaluated at interpolated angles of attack satisfying a common normal-force requirement. A feasibility-aware objective combines drag and aerodynamic efficiency with residual pitching moment, static stability, local control demand, geometric compactness, and normal-force-derivative retention. The proposed and Vasile-type formulations are compared under identical design bounds, aerodynamic evaluation, PSO settings, and computational budget. Across 15 paired runs, the proposed formulation yields lower drag and higher lift-to-drag ratio in every pair. For the median-representative pair, drag decreases by 8.13% and lift-to-drag ratio increases by 8.85% relative to the Rose baseline configuration; the corresponding improvements over the Vasile-type design are 7.98% and 8.67%, with all feasibility requirements satisfied.

Keywords: Aerodynamic optimization; Missile DATCOM; Particle swarm optimization; Multi-component objective function; Static margin; Normal-force derivative.

1. INTRODUCTION

Preliminary aerodynamic configuration design requires exploring a broad geometric space before higher-fidelity analysis is warranted. Changes in lifting-surface location, span, and chord distribution jointly affect drag, normal-force generation, pitching moment, static stability, and control demand; single-coefficient optimization may therefore yield an efficient but physically unsuitable configuration. Missile DATCOM supports this stage by rapidly estimating aerodynamic coefficients and stability derivatives [1]. Evolutionary, swarm-based, and parameter-space methods have been applied to missile and guided-vehicle design [2-7], including the PSO-Missile DATCOM procedure of Vasile et al. based on drag, lift-to-drag ratio, and static margin [6].

These studies establish the feasibility of optimizer-assisted design, but the selected configuration remains sensitive to the evaluation criterion. Weighted aggregation requires consistent normalization and explicit interpretation of design preferences [8]. Fixed-angle evaluation may also compare geometries at different normal-force levels, allowing apparent efficiency gains to conceal degraded force capability, pitching-moment behavior, or control demand. The central problem is therefore to compare candidate geometries under a common force requirement while preserving the supporting physical characteristics.

PSO is retained as the common search engine for the proposed and Vasile-type formulations to maintain continuity with the closest related study and avoid confounding objective-function effects with optimizer differences [6]. It is compatible with the present eleven-variable, bounded, continuous, and gradient-free problem [9-11]; although competitive performance against a basic genetic algorithm has been reported, no universal superiority is claimed [12, 13]. Applied to the Rose baseline configuration [14], the proposed framework evaluates each candidate at an interpolated angle

satisfying the prescribed normal-force requirement and ranks feasible designs using aerodynamic efficiency, residual pitching-moment magnitude, static margin, local control demand, geometric compactness, and normal-force-derivative retention. The contribution is this force-conditioned, feasibility-aware objective architecture and its controlled comparison with the Vasile-type formulation under identical design, simulation, and search conditions.

2. PROBLEM FORMULATION AND OPTIMIZATION FRAMEWORK

The study compares two aerodynamic objective formulations under identical search and simulation conditions. For branch $b \in \{P,V\}$, denoting the proposed and Vasile-type formulations, respectively: $X_b^* = \arg\min_{X\in\Omega} J_b(X)$, where X is the geometric design vector and Ω is the admissible design domain. Both branches use the same Missile DATCOM evaluator, design bounds, feasibility conditions, PSO parameters, paired random seeds, and evaluation budget; only the branch score differs. This controlled design isolates the effect of objective-function formulation.

2.1. Geometry and aerodynamic evaluator

The Rose baseline (Brumby UAV) configuration adopted in this study follows the geometry and Missile DATCOM FINSET representation reported by Rose, with FINSET1 representing the main lifting surface and FINSET2 the twin vertical stabilizers [14]. This configuration provides a traceable and reproducible reference for defining the eleven-variable design domain and for the controlled comparison of the two objective formulations. The design vector is

$$X = \left[x_{LE,w}, s_{w,m}, s_{w,t}, c_{w,r}, c_{w,m}, c_{w,t}, x_{LE,v}, s_{v,r}, s_{v,t}, c_{v,r}, c_{v,t} \right]^T \quad (1)$$

where x_{LE}, s, and c denote the axial leading-edge coordinate, the spanwise station measured from the vehicle centerline, and the local chord, respectively. The subscripts w and v identify FINSET1, the main lifting surface, and FINSET2, the twin vertical stabilizers, respectively. The subscripts r, m, and t denote the root or inner station, the intermediate or mid-break station, and the tip or outer station.

The eleven variables and their local bounds about the Rose baseline geometry are shown in Figure 1 and Table 1. Airfoil data, body geometry, panel orientation, sweep convention, and control-surface definitions remain fixed.

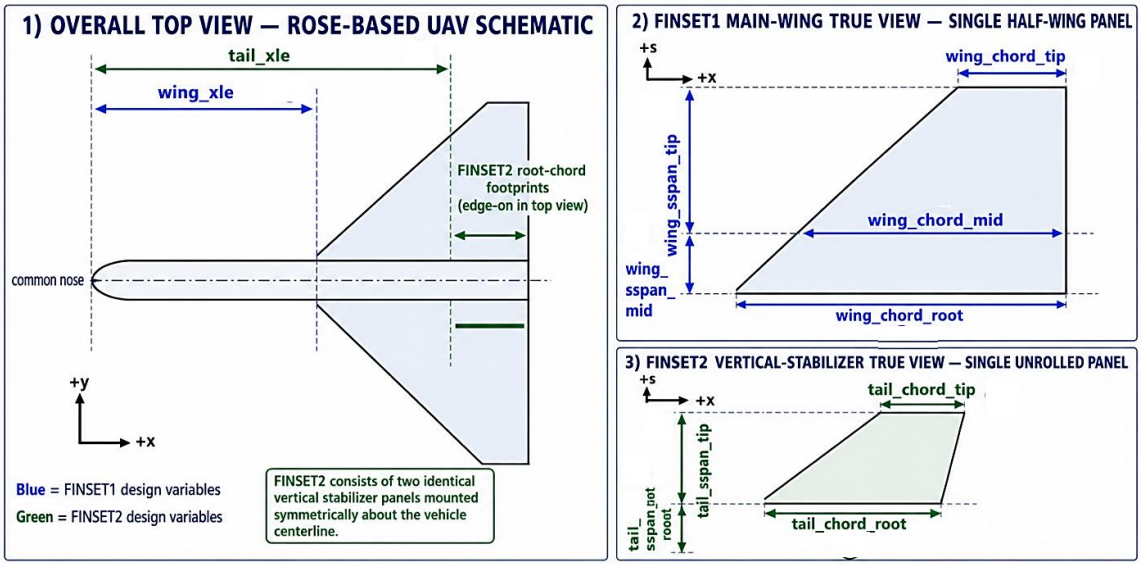


Figure 1. *Rose baseline geometry and the eleven Missile DATCOM design variables.*

Table 1. *Optimization variables and their bounds.*

Variable	Name in vector X	Rose value (m)	Lower bound (m)	Upper bound (m)
wing_xle	$x_{LE,w}$	0.9700	0.9000	1.0400
wing_sspan_mid	$s_{w,m}$	0.2660	0.2400	0.3000
wing_sspan_tip	$s_{w,t}$	1.0096	0.8600	1.1200
wing_chord_root	$c_{w,r}$	1.0033	0.8500	1.1500
wing_chord_mid	$c_{w,m}$	0.8048	0.6500	0.9500
wing_chord_tip	$c_{w,t}$	0.2500	0.1800	0.3400
tail_xle	$x_{LE,v}$	1.5700	1.3600	1.6500
tail_sspan_root	$s_{v,r}$	0.2660	0.2400	0.3200
tail_sspan_tip	$s_{v,t}$	0.6726	0.5500	0.8000
tail_chord_root	$c_{v,r}$	0.4000	0.3200	0.4800
tail_chord_tip	$c_{v,t}$	0.1952	0.1400	0.2500

The box bounds in Table 1 already enforce span-station ordering and nondegenerate tip/root chord ratios. The following coupled conditions therefore retain only the additional restrictions that further reduce the present admissible domain:

$$c_{w,m}/c_{w,r} \le 1.05; \qquad x_{LE,v} + c_{v,r} \le 1.97 \tag{2}$$

The first condition limits excessive chord expansion at the FINSET1 mid-break, whereas the second keeps the FINSET2 root-chord trailing edge within the aft geometric limit defined by the Rose baseline configuration. These are local engineering guards for the present design family rather than universal aerodynamic bounds.

Each valid vector is written into a common DATCOM deck, after which the required static and control tables are parsed [1, 6]. Cases with missing tables or non-finite metrics are rejected. The same writer, executable, parser, and post-processor are used for both branches.

The geometric area ratio is evaluated from the total two-sided planform area of FINSET1 and FINSET2:

$$r_A(X) = A_{aero}(X)/A_{aero,Rose} \tag{3}$$

2.2. Force-conditioned operating point and derived metrics

A fixed angle of attack does not impose the same normal-force demand on different geometries. Each configuration is therefore evaluated at an angle satisfying:

$$C_{N,req} = mg\cos\gamma/\left(0.5\rho V^2 S_{ref}\right) = 0.03527 \tag{4}$$

where $m = 22.8543\ kg$, $\rho = 1.229\ kg/m^3$, $V = 90.9144\ m/s$, $g = 9.81\ m/s^2$, $\gamma = 0^o$, and $S_{ref} = 1.2517\ m^2$.

Rose's straight-and-level trimmed Case 1 gives $V = 90.9144$ m/s and $\beta = 0°$; using the speed of sound $a = 340.29$ m/s adopted in Rose's 6DOF code gives $M = 0.26717 \approx 0.267$ [14]. This condition is used here as a nominal comparison point rather than as the full Brumby flight envelope.

Let α_j and α_{j+1} bracket $C_{N,req}$. The operating angle is obtained by linear interpolation:

$$\alpha_{lb}(X)=\alpha_j+\frac{C_{N,req}-C_N(\alpha_j;X)}{C_N(\alpha_{j+1};X)-C_N(\alpha_j;X)}(\alpha_{j+1}-\alpha_j) \tag{5}$$

The same interpolation fraction is applied to C_D, C_L, C_N, and C_M. A configuration without a bracketed crossing is classified as infeasible rather than evaluated by extrapolation.

The Missile-DATCOM-reported derivative tables are interpolated at the same operating angle:

$$C_{N\alpha}(X)=\text{interp}[CNA(\alpha),\alpha_{lb}],\ C_{M\alpha}(X)=\text{interp}[CMA(\alpha),\alpha_{lb}],\ SM(X)=-C_{M\alpha}(X)/C_{N\alpha}(X) \tag{6}$$

Normal-force-derivative retention is defined as:

$$r_{C_{N\alpha}}(X)=C_{N\alpha}(X)/C_{N\alpha,Rose} \tag{7}$$

The FINSET1 control metric combines the two stored symmetric-panel perturbations:

$$C_{M\delta}=\frac{C_M(\alpha_{lb};\delta_1=-5^o,\delta_2=0^0)+C_M(\alpha_{lb};\delta_1=0^o,\delta_2=+5^o)-2C_M(\alpha_{lb};\delta_1=0^o,\delta_2=0^o)}{5^o} \tag{8}$$

$$\delta_{req}=-C_M(\alpha_{lb},0^o)/C_{M\delta},\quad e_\delta=|\delta_{req}|/25^o \tag{9}$$

Here, δ_1 and δ_2 refer to the two symmetric FINSET1 panels. Owing to their opposite local sign conventions, δ_1 =−5° and δ_2 =+5° represent moment contributions in the same global pitching direction; Equation (8) therefore estimates their combined local control derivative. Meanwhile, 25° is the prescribed control-travel limit. Equations (5)–(9) provide a force-conditioned local assessment; they do not constitute complete trim, which would require simultaneous force and moment equilibrium and a realizable actuator state [15].

2.3. Feasibility and objective functions

The raw metrics are mapped to [0,1] using:

$$clip(z)=\min\{\max(z,0),1\} \tag{10}$$

Let $E=C_L/C_D$ and $e_N=\left(|C_N(\alpha_{lb})-C_{N,req}|\right)/C_{N,req}$. The normalized components are

$$\begin{aligned}
&S_D=clip\left(\frac{C_{D,Rose}-C_D}{C_{D,Rose}-0.0095}\right),\ S_E=clip\left(\frac{E-E_{Rose}}{3.60-E_{Rose}}\right),\ S_N=clip\left(1-\frac{e_N}{0.50}\right),\\
&S_M=clip\left(1-\frac{|C_M(\alpha_{lb},0^o)|}{0.080}\right),\ S_\delta=clip\left(\frac{0.80-e_\delta}{0.80}\right),\\
&S_{SM}=clip\left(1-\frac{|SM-0.12|}{0.12}\right),\ S_G=clip\left(\frac{1-r_A}{1-0.92}\right),\ S_{C_{N\alpha}}=clip\left(\frac{r_{C_{N\alpha}}-0.9}{0.98-0.9}\right).
\end{aligned} \tag{11}$$

where $C_{D,Rose}$ = 0.0125510, E_{Rose} = 2.80977.

The drag and efficiency scores are therefore referenced to the Rose baseline configuration, while C_D= 0.0095 and $E=3.60$ are prescribed upper-performance anchors fixed before the paired runs.

The proposed and reference branch scores are

$$S_P(X)=0.32S_D+0.32S_E+0.06S_N+0.05S_M+0.05S_{SM}+0.06S_\delta+0.04S_G+0.10S_{C_{N\alpha}} \tag{12}$$

The weights were assigned after all component scores were normalized to [0,1]. A total weight

of 0.64 was allocated equally to drag and aerodynamic efficiency because they are the two primary design objectives, while the remaining 0.36 ranks feasible candidates using the supporting force, moment, stability, control-demand, and compactness metrics. The weights were fixed before the paired runs and represent a declared design preference rather than universal physical constants [8]. Changing the weights can change the selected geometry because it changes the ranking of feasible candidates; weight-invariant optimality is therefore not claimed.

For Vasile-type branch, the score is calculated as [6]:

$$S_V(X) = (2/7)S_E + (1/7)S_D + (4/7)S_{SM} \tag{13}$$

The term Vasile-type denotes retention of the relative three-component weighting structure; the present geometry, normalization, force-conditioned operating point, and common feasibility envelope are used in both branches.

Before either branch score is used for aerodynamic ranking, the candidate must satisfy the common feasibility requirements:

$$0.085 \le SM \le 0.130, \quad r_{C_{N\alpha}} \ge 0.95, \quad r_A \ge 0.90, \quad S_\delta \ge 0.90 \tag{14}$$

together with a valid bracketed crossing of $C_N = C_{N,req}$, complete Missile DATCOM tables, and finite aerodynamic metrics. A candidate without a bracketed crossing is declared infeasible; neither extrapolation nor nearest-node substitution is used for aerodynamic ranking.

Only violated requirements contribute to V_{common}. Violations of the lower and upper static-margin limits, normal-force-derivative retention, aerodynamic-area ratio, and local control-demand score are normalized by 0.02, 0.03, 0.05, 0.05, and 0.05, respectively, and squared before aggregation. Failure to obtain a bracketed operating point or complete finite DATCOM data incurs a unit violation. The same definition and scaling are applied to both branches.

The scalar minimized by PSO is

$$J_b(X) = 1000V_{common}(X) - S_b(X), \quad b \in \{P,V\} \tag{15}$$

For feasible candidates, V_{common} = 0, and minimizing J_b is equivalent to maximizing the corresponding branch score. The penalty coefficient was selected so that infeasible candidates could not outrank feasible candidates in the recorded searches. Geometrically malformed configurations are rejected before Missile DATCOM execution and assigned $J_b = 10^6$. This feasibility-first treatment follows established constraint-handling practice in evolutionary optimization [16].

2.4. PSO realization and controlled comparison

A global-best PSO with inertia weighting is used [9, 17]:

$$V_i^{k+1} = \omega V_i^k + c_1 R_{1,i}^k \odot \left(P_i^k - X_i^k\right) + c_2 R_{2,i}^k \odot \left(G^k - X_i^k\right) \tag{16}$$

$$X_i^{k+1} = \mathrm{B}_\Omega\left(X_i^k + V_i^{k+1}\right) \tag{17}$$

Each particle position is the geometry in Eq. (1), and P_i^k and G^k are selected using the complete objective in Equation (15), not an individual aerodynamic coefficient. Thus, each evaluation follows

$$X_i^k \to DATCOM \to \alpha_{lb} \to V_{common}, S_b \to J_b \to P_i^{k+1}, G^{k+1} \tag{18}$$

The settings are $\omega = 0.55$, $c_1 = 1.35$, $c_2 = 1.55$, $V_{\max,j} = 0.16\left(x_{j,\max} - x_{j,\min}\right)$.

The first particle is initialized at the Rose baseline geometry; the remaining particles are

uniformly distributed within the box bounds. Initial velocities are uniformly sampled in $\left[-0.5V_{\max,j}, 0.5V_{\max,j}\right]$. Velocities are clipped to $\pm V_{\max,j}$, and positions leaving the box are returned to the nearest bound before the coupled geometric checks are applied.

Each branch uses 20 particles, 60 iterations, and 15 paired seeds, corresponding to 18,000 evaluations per branch and 36,000 evaluations in total. The 15 paired seeds provide a repeatability sample within the fixed evaluation budget, while matched initialization removes between-branch swarm initialization as a confounding factor. For every seed, the two branches start from matched random initialization and use identical search and aerodynamic conditions. Their trajectories diverge only because S_P and S_V rank the same evaluated geometries differently. Conclusions are therefore based on paired physical metrics across all seeds, not on the raw magnitudes of J_P and J_V or on a single selected run [18].

3. RESULTS AND DISCUSSION

The results are examined at two levels. The complete set of paired PSO runs is first used to determine whether the effect of the objective formulation is repeatable under stochastic initialization. A median-representative pair is then examined to relate the statistical result to the corresponding aerodynamic behavior. This separation avoids drawing conclusions from a single favorable solution.

3.1. Paired optimization results

At $M = 0.267$, $\beta = 0^o$, the 15 paired runs described in Section 2.4 were used for the physical-metric comparison. For every seed, the proposed and Vasile-type searches used the same initial swarm, design domain, PSO settings, aerodynamic evaluator, feasibility conditions, and computational budget. For paired seed s, define

$$\Delta C_D^s = C_{D,P}^s - C_{D,V}^s, \quad \Delta E^s = E_P^s - E_V^s \tag{19}$$

where $E = C_L/C_D$. Negative ΔC_D and positive ΔE favor the proposed formulation.

The proposed branch produced lower C_D and higher C_L/C_D in all 15 paired runs. The median paired effects were:

$$\text{median}\left(\Delta C_D\right) = -0.00100, \quad \text{median}\left(\Delta E\right) = +0.2450$$

For each metric, all 15 paired differences had the favorable sign. The consistency of the result across the complete seed set is more informative than the objective histories themselves because J_P and J_V have different component structures and numerical scales. The paired result demonstrates that, under the declared design domain and search budget, the proposed score systematically changes the PSO ranking toward lower drag and higher aerodynamic efficiency.

This improvement cannot be attributed to unequal admissible domains. All final solutions used in the comparison satisfy the same requirements on static margin, normal-force-derivative retention, aerodynamic area, local control demand, operating-point validity, and DATCOM-data completeness.

3.2. Representative feasible trade-off

Seed 71009 minimizes the normalized distance to the four branch medians of C_D and C_L/C_D and is therefore used only as a representative pair. It is used to illustrate typical behavior rather than the largest favorable Proposal–Vasile difference.

The percentage columns report signed relative differences rather than universal improvement measures. In particular, the + 46.80% difference in $|C_M|$ relative to Rose corresponds to an absolute difference of only 0.00095 because the Rose reference value is close to zero.

Table 2. *Representative aerodynamic metrics at the force-conditioned operating points.*

Indicator	Proposal	Vasile-type	Rose baseline	Proposal vs. Vasile (%)	Proposal vs. Rose (%)
C_D	0.011530	0.012530	0.012551	**-7.98**	**-8.13**
C_L/C_D	3.0585	2.8144	2.8098	**+8.67**	**+8.85**
Static margin	0.1132	0.1200	0.0864	-5.67	+31.02
$C_{N\alpha}$ retention	1.0334	1.0401	1.0000	-0.64	+3.34
Aerodynamic-area ratio	0.9195	1.0334	1.0000	-11.02	-8.05
$\alpha_{lb}(\deg)$	0.5303	0.5303	0.5510	0.00	-3.76
Local FINSET1 control-demand score, S_δ	0.9468	0.9421	0.9492	+0.50	-0.25
$\left\|C_M\left(\alpha_{lb}, \delta = 0^o\right)\right\|$	0.00298	0.00324	0.00203	-8.02	+46.80

As summarized in Table 2, the proposed configuration improves both primary aerodynamic objectives relative to the Vasile-type and Rose references.

The proposed configuration also uses 8.05% less aerodynamic-surface area than Rose, whereas the Vasile-type design uses 3.34% more. The drag reduction is therefore associated partly with a more compact planform. However, it is not obtained through a loss of local force sensitivity: the proposed configuration retains $r_{C_{N\alpha}}$ =1.0334, corresponding to a 3.34% increase relative to Rose, and satisfies the prescribed normal-force requirement at a slightly lower angle than the Rose baseline.

The proposed solution satisfies all common feasibility requirements and provides the strongest efficiency–compactness trade-off. It does not dominate every individual metric: the Vasile-type configuration is closer to the preferred static margin and has slightly higher $C_{N\alpha}$ retention, whereas Rose has the smallest residual pitching-moment magnitude.

3.3. Aerodynamic behavior near the operating point

Figure 2 uses $0^o \le \alpha \le 1.2^o$ only as a local display window to magnify the three force-conditioned operating points at 0.5303°, 0.5303°, and 0.5510°. This interval is not an optimization constraint or a Missile DATCOM angle-of-attack limit; it lies entirely within the stored 0°–2° bracket containing all three operating points.

The proposed configuration retains the lowest C_D throughout the displayed interval and the highest C_L/C_D over the positive-angle neighborhood containing the operating points. Figure 2(c) shows that all three markers lie on the same prescribed level, $C_N = C_{N,req}$. Thus, the proposed efficiency advantage is not created by evaluating it at a lower normal-force demand. The equal Proposal and Vasile-type values of α_{lb} are obtained independently from their respective $C_N(\alpha)$ curves and coincide only at the reported precision.

The minima in Figure 2(d) arise from zero crossings of the interpolated signed C_M at $\delta = 0^o$. They are not complete trim points: at those angles, the normal-force requirement is not simultaneously satisfied. Conversely, at α_{lb}, the required normal force is achieved but a finite residual pitching moment remains. Because the panel displays $|C_M|$, its slope must not be used to infer $C_{M\alpha}$ or static stability.

Taken together, the paired runs, representative metrics, and local aerodynamic trends provide mutually consistent evidence. The proposed multi-component objective changes the personal/global best histories of the same PSO search and directs it toward a configuration with lower drag and higher aerodynamic efficiency, without relaxing the common normal-force or feasibility conditions.

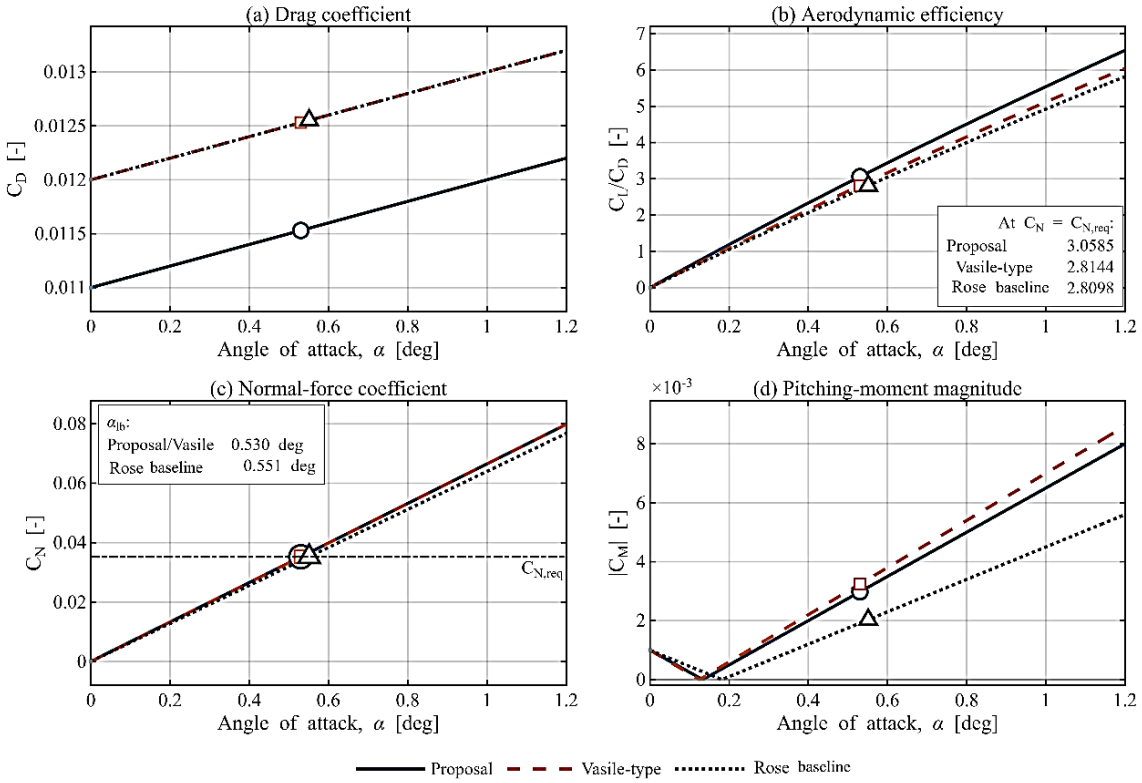


***Figure 2**. Representative aerodynamic characteristics in the force-conditioned operating-point neighborhood, $0^o \le \alpha \le 1.2^o$, at the selected Missile DATCOM condition $M = 0.267$.*

4. CONCLUSIONS

This study developed a preliminary aerodynamic configuration optimization framework coupling PSO with Missile DATCOM through a force-conditioned, feasibility-aware multi-component objective. Candidate geometries are compared at independently interpolated angles satisfying the same normal-force requirement and are ranked using aerodynamic efficiency, residual pitching-moment magnitude, static margin, local control demand, geometric compactness, and normal-force-derivative retention. The contribution therefore lies in the objective-function architecture and the controlled comparison protocol rather than in PSO or weighted aggregation alone.

Under identical design bounds, feasibility requirements, aerodynamic evaluation, PSO settings, paired seeds, and computational budget, the proposed formulation produced lower C_D and higher C_L/C_D in all 15 paired runs. For the median-representative pair, C_D decreased by 8.13% and C_L/C_D increased by 8.85% relative to the Rose baseline configuration; the corresponding improvements over the Vasile-type design were 7.98% and 8.67%. All prescribed feasibility requirements remained satisfied. These results demonstrate a more favorable preliminary aerodynamic trade-off under the declared weighting structure and design domain. The quantitative gains are conditional on the Missile DATCOM model and the nominal

$M = 0.267$, $\beta = 0°$ condition and do not constitute cross-solver or full-envelope validation. Extension to $\beta \neq 0°$ requires lateral-directional stability and control metrics. Future work will therefore include Digital DATCOM cross-checking and higher-fidelity CFD validation, consistent with numerical aerodynamic assessment approaches applied to related flying-body configurations [19, 20]. Multi-condition optimization, coupled trim, 6DOF assessment, and actuator constraints will also be addressed.

REFERENCES

[1]. W. B. Blake, "*Missile Datcom: User's Manual - 1997 FORTRAN 90 Revision*", (1998).

[2]. C. Tanil, "*Optimal external configuration design of a missile*", (2009).

[3]. S. Y. Nabavi and S. H. Pourtakdoust, "*Aerodynamic shape optimization of unguided projectiles using Ant Colony Optimization and Genetic Algorithm*", Vol. 2, pp. 698–706, (2006).

[4]. T. Tuan, N. Thăng and N. Ngoc Dien, "*Multi-objective optimization of the aerodynamic shape of the front fuselage of a controlled flying aircraft by parameter space investigation*", Journal of Mechanical Engineering Research and Developments, Vol. 44, pp. 101–111, (2021).

[5]. S. M. Zandavi and S. H. Pourtakdoust, "*Multidisciplinary design of a guided flying vehicle using simplex nondominated sorting genetic algorithm II*", Structural and Multidisciplinary Optimization, Vol. 57, pp. 705–720, (2018).

[6]. J. D. Vasile, J. T. Bryson and F. E. Fresconi, "*Aerodynamic design optimization of long range projectiles using Missile DATCOM*", AIAA Scitech 2020 Forum, (2020).

[7]. G. P. Zhang, Z. Z. Liao, C. Y. Duan and P. Wang, "*Optimal design of configuration change program for tactical missile with morphing wings*", Applied Mechanics and Materials, Vol. 101–102, pp. 410–413, (2011).

[8]. R. T. Marler and J. S. Arora, "*The weighted sum method for multi-objective optimization: New insights*", Structural and Multidisciplinary Optimization, Vol. 41, No. 6, pp. 853–862, (2010). DOI: 10.1007/s00158-009-0460-7.

[9]. J. Kennedy and R. Eberhart, "*Particle swarm optimization*", Proceedings of ICNN'95 - International Conference on Neural Networks, Vol. 4, pp. 1942–1948, (1995). DOI: 10.1109/ICNN.1995.488968.

[10]. G. Venter and J. Sobieszczanski-Sobieski, "*Multidisciplinary optimization of a transport aircraft wing using particle swarm optimization*", Structural and Multidisciplinary Optimization, Vol. 26, No. 1, pp. 121–131, (2004). DOI: 10.1007/s00158-003-0318-3.

[11]. J. F. Schutte, J. A. Reinbolt, B. J. Fregly, R. T. Haftka and A. D. George, "*Parallel global optimization with the particle swarm algorithm*", International Journal for Numerical Methods in Engineering, Vol. 61, No. 13, pp. 2296–2315, (2004). DOI: 10.1002/nme.1149.

[12]. R. Hassan, B. Cohanim, O. de Weck and G. Venter, "*A comparison of particle swarm optimization and the genetic algorithm*", 46th AIAA/ASME/ASCE/AHS/ASC Structures, Structural Dynamics and Materials Conference.

[13]. D. Wolpert and W. Macready, "*No free lunch theorems for optimization*", IEEE Transactions on Evolutionary Computation, Vol. 1, pp. 67–82, (1997). DOI: 10.1109/4235.585893.

[14]. D. Rose, "*Aerodynamic modeling of an unmanned aerial vehicle using a computational fluid dynamics prediction code*", (2009).

[15]. B. Etkin and L. D. Reid, "*Dynamics of Flight: Stability and Control*", John Wiley & Sons, (1995).

[16]. C. A. Coello Coello, "*Theoretical and numerical constraint-handling techniques used with evolutionary algorithms: A survey of the state of the art*", Computer Methods in Applied Mechanics and Engineering, Vol. 191, No. 11, pp. 1245–1287, (2002). DOI: 10.1016/S0045-7825(01)00323-1.

[17]. Y. Shi and R. Eberhart, "*A modified particle swarm optimizer*", Evolutionary Computation Proceedings, Vol. 890, pp. 69–73, (1998).

[18]. Q. Liu et al., "*Paradoxes in numerical comparison of optimization algorithms*", IEEE Transactions on Evolutionary Computation, Vol. 24, No. 4, pp. 777–791, (2019).

[19]. T. T. Hung, N. T. Minh and D. C. Truong, *"Aerodynamic characteristics of flow over boat-tail models at subsonic and supersonic conditions",* Journal of Military Science and Technology, No. 75A, pp. 60–69, (2021). DOI: 10.54939/1859-1043.j.mst.75A.2021.60-69.

[20]. L. H. Ban, N. N. Quy, N. H. Minh, D. N. Ke and N. Q. Luong, *"Investigating and evaluating the influence of drag ring diameter on the range of an ungovernable flying device in standard conditions",* Journal of Military Science and Technology, No. 78, pp. 159–165, (2022). DOI: 10.54939/1859-1043.j.mst.78.2022.159-165.

TÓM TẮT

Tối ưu sơ bộ cấu hình khí động học sử dụng PSO với hàm mục tiêu đa thành phần

Bài báo đề xuất khung tối ưu sơ bộ cấu hình khí động kết hợp PSO với Missile DATCOM. Mỗi cấu hình Rose/Brumby gồm 11 biến được đánh giá tại góc tấn nội suy thỏa mãn cùng yêu cầu lực pháp tuyến. Hàm mục tiêu có xét miền khả thi kết hợp hiệu quả khí động với các yêu cầu về mô men, ổn định, chỉ số nhu cầu điều khiển cục bộ, hình học và đạo hàm lực pháp tuyến. Hai hàm mục tiêu đề xuất và kiểu Vasile được so sánh trong cùng điều kiện thiết kế và tính toán. Qua 15 cặp chạy, phương pháp đề xuất luôn đạt hệ số cản thấp hơn và tỷ số lực nâng trên lực cản cao hơn. Với cặp đại diện gần trung vị, mức cải thiện so với Rose là 8,13% và 8,85%; so với Vasile là 7,98% và 8,67%, trong khi các điều kiện khả thi vẫn được bảo đảm.

Từ khoá: Tối ưu khí động; Missile DATCOM; Tối ưu bầy đàn; Hàm mục tiêu đa thành phần; Độ dự trữ ổn định tĩnh; Đạo hàm lực pháp tuyến.